Towards design for precision additive manufacturing
A simplified approach for detecting heat accumulation

Ranjan, Rajit; Ayas, Can; Langelaar, Matthijs; van Keulen, Fred

Publication date
2018

Document Version
Final published version

Published in
Proceedings of the ASPE and EUSPEN Summer Topical Meeting

TOWARDS DESIGN FOR PRECISION ADDITIVE MANUFACTURING: A SIMPLIFIED APPROACH FOR DETECTING HEAT ACCUMULATION

Rajit Ranjan[1], Can Ayas[1], Matthijs Langelaar[1], and Fred van Keulen[1]
[1]Precision and Microsystems Engineering (PME)
Delft University of Technology
Delft,The Netherlands

INTRODUCTION

Selective laser melting (SLM) is a powder based metal additive manufacturing (AM) process that offers an unprecedented form freedom. Therefore, it is considered as an ideal enabling technology for topology optimized designs. The latter are typically complex in layout, but superior in performance. However, state of the art SLM machines cannot realize the dimensional accuracies required for high-precision components. One important issue leading to dimensional inaccuracy is the rapid heating-cooling of layers because of laser induced heat. As the laser melts the powder at the uppermost layer, heat diffuses towards the base plate which acts as a heat sink. It is well known that certain design features (e.g. overhangs and thin sections) can obstruct heat flow and cause local heat accumulation which leads to poor surface finish and undesired mechanical properties [1]. In literature, it has been suggested to use geometry based design guidelines which can sometimes become insufficient for avoiding heat accumulation [2]. Therefore, it would be beneficial to detect such features early during the design stage and thereby develop next generation topology optimization (TO) methods which could serve as an ideal design tool for precision AM industry.

In order to address thermal aspects of AM into a TO framework, an appropriate AM process model is required. This becomes problematic because a high fidelity AM process model is computationally very expensive and integrating it within a gradient-based TO framework becomes even more cumbersome [3]. Therefore, in this research, a physics based yet highly simplified approach is proposed in order to identify zones of heat accumulation in a given design. The computational gain offered by the simplification, makes it feasible to integrate the heat accumulation detection scheme within a TO framework.

The focus of this paper is on a simplified heat accumulation detection procedure, which is essential to ultimately realize a TO scheme accounting for thermal AM aspects. Aside from its use in a TO process, it can be independently used for analyzing AM designs, manual design improvements and determining optimal build orientations. In this paper, only the heat accumulation detection method is presented and its integration within a TO framework will be discussed in a separate paper.

There are two main simplifications made in this research which assists in reducing the computational cost associated with thermal analysis of AM designs. First simplification is to perform the thermal analysis only in the vicinity of the AM layer which is being deposited. This is motivated by the fact that the local geometry of only few previously molten layers have a significant effect on the *initial* cooling rate of the newly deposited layer [4]. The second simplification is to utilize a steady state thermal response, instead of transient, in order to predict heat accumulation. For this purpose, a physics based conceptual understanding is developed which enables estimation of spatially averaged transient thermal behavior of a local geometry just from its steady state response.

HEAT ACCUMULATION DETECTION: CONCEPTUAL UNDERSTANDING

It is well known that the topology of a structure has an influence on the heat flow inside it. Hence, different geometrical features in an AM design facilitate/obstruct heat flow during the AM process in a different manner. In this work we explore the possibility to approximately quantify, and hence compare, different geometries from the viewpoint of heat accumulation. For this purpose, first the concepts of thermal conductance and time constants are studied.

Thermal Conductance

Thermal conductance C is defined as the measure of a structure to conduct heat [5]. It is also equivalent to the reciprocal of thermal resistance. For an 1D case, thermal conductance is defined as

$$C = \frac{Q}{\Delta T} = \frac{k\mu}{L}, \tag{1}$$

where k represents thermal conductivity of the material, Q is the rate of heat transfer across a 1D rod with length L and cross-section area μ, and a steady state temperature difference of ΔT is achieved across the two ends of the rod. It is to be noted that thermal conductance is property of a structure as this definition addresses the geometry of the object by including the length and cross section parameters.

Figure 1 shows a 2D shape which is subjected to a heat load Q at its top edge while the bottom edges are fixed at temperature T_o with all other boundaries as thermally insulated. A steady state temperature field $T(x, y)$ is obtained which depends on described boundary conditions, material properties and topology itself. In order to quantify the conductive capability of this 2D geometry, we define the average thermal conductance as

$$\bar{C} = \frac{Q}{2(\bar{T}_{\text{ss}} - T_o)}. \tag{2}$$

Here, $\bar{T}_{\text{ss}}$ is the area averaged temperature which is calculated as

$$\bar{T}_{\text{ss}} = \frac{1}{A}\int\int T(x, y)dxdy, \tag{3}$$

where A is the area of the 2D object. Equivalently, in 3D a volume average is used. The boundary conditions used here are motivated by the AM process itself, where every design feature experiences a sudden heat load at the top and previously manufactured parts along with the base plate act as a heat sink. Also, powder surrounding the part has a very low thermal conductivity because of which the condition of thermal insulation has been considered for all other sides. The

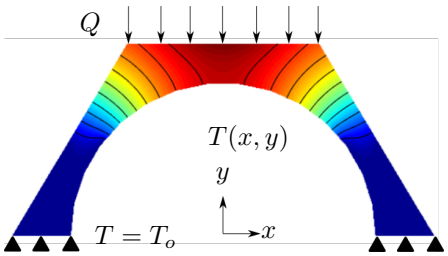

FIGURE 1. Steady state temperature field $T(x, y)$ for a 2D geometry with heat load Q acting on the top edge, bottom edges are at a fixed temperature T_o and all other edges are thermally insulated.

factor of 2 in the denominator of Eq. (2), is introduced in order to conform to the 1D definition of conductance given by Eq. (1), since for 1D case, $\Delta T = 2(\bar{T}_{\text{ss}} - T_o)$. Next, thermal conductance estimated from the highly simplified steady-state analysis is used to predict the heating/cooling rates of local topologies. This is motivated by the fact that post solidification cooling rates determine heat accumulation behavior and have a significant effect on micro-structural evolution [6]. In order to quantify heating/cooling rate we choose to study the time constant of the transient thermal response.

Thermal time constant

First, an expression is introduced for the average time constant in a 1D setting which is subsequently extended to 2D and 3D bodies.

1D heat transfer: Analytical study

Consider a 1D rod of length L subjected to heat flux ϕ at $x = L$ and ideal heat sink boundary condition at $x = 0$. The 1D heat equation reads

$$\frac{\partial T}{\partial t} = \alpha \frac{\partial^2 T}{\partial x^2} \tag{4}$$

Boundary conditions are given as

$$k\frac{\partial T}{\partial x}\bigg|_{x=L} = -\phi, \tag{5}$$

$$T(0, t) = 0 \quad \text{for} \quad t \geq 0, \tag{6}$$

and the initial condition is taken as

$$T(x, 0) = 0 \quad \text{for} \quad x \in [0, L]. \tag{7}$$

Here, t is time, α is thermal diffusivity and x is position. Thermal diffusivity is given as $k/\rho c$ where ρ and c are mass density and specific heat, respectively. Using the method of separation of variables, the temperature distribution $T(x,t)$ as function of position and time is found and average temperature over the entire length of rod is calculated as

$$\bar{T}(t) = \frac{1}{L}\int_0^L T(x,t)dx. \tag{8}$$

Substituting the closed form solution of Eq. (4-7) in Eq. (8) and integrating, we find a converging infinite series given as

$$\bar{T}(t) = \frac{\phi L}{2k}\left[1 - \frac{32}{\pi^3}\sum_{n=1}^{\infty}\frac{(-1)^{n+1}}{(2n-1)^3}e^{-(\frac{2n-1}{2})^2\frac{\pi^2\alpha t}{L^2}}\right]. \tag{9}$$

If we consider only the first term of the series, spatially average temperature can be approximated as

$$\bar{T}(t) = \frac{\phi L}{2k}\left[1 - \frac{32}{\pi^3}e^{-\frac{\pi^2\alpha t}{4L^2}}\right]. \tag{10}$$

Eq. (10) represents an exponential rise of $\bar{T}(t)$ for which time constant is given as

$$\bar{\tau} = \frac{4L^2}{\pi^2}\frac{1}{\alpha} = \frac{4L^2}{\pi^2}\frac{\rho c}{k}. \tag{11}$$

As expected, the average time constant is proportional to the heat capacity and inversly proportional to thermal conductivity.

Estimation of average time constant using 1D analogy

In this section, expression found for average time constant $\bar{\tau}$ for an 1D case is utilized for estimating that for 2D and 3D bodies. Figure 2 shows a 3D body (labeled as A) with volume V which is subjected to heat energy Q per unit time and bottom surface is fixed at $T = T_o$. We first define thermal capacitance for this body as

$$\lambda = V\rho c, \tag{12}$$

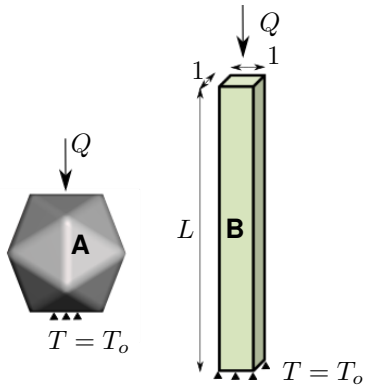

FIGURE 2. Equivalence of a 3D body (A) to a simplified body (B) with equal thermal capacitance and conductance.

analogous to the relation between conductivity and conductance c.f. Eq. (1). Next, we consider an imaginary body B with length L and unit width and depth such that both A and B have same thermal capacitance λ and conductance $\bar{C}$ when subjected to same boundary conditions. This is motivated by the fact that body B can be characterized by 1D understanding developed in the previous section and thermal equivalence between body A and B enables prediction of lumped thermal behavior of body A by computing that of body B. Equal thermal capacitance implies that both the bodies have same volume (assuming same specific heat and density) i.e.

$$L \cdot 1 \cdot 1 = V. \tag{13}$$

Next, equating the thermal conductance for both bodies and using Eq. (1) for body B, following expression can be written

$$\bar{C}_A = \bar{C}_B = \frac{k_B\mu}{L}, \tag{14}$$

where k_B is thermal conductivity of body B. As normal cross section area for body B is unity i.e. $\mu = 1$, k_B can be rewritten as

$$k_B = \bar{C}_A L. \tag{15}$$

Substituting found value of k_B from Eq. (15) into Eq. (11), and using Eq. (13), we find an estimate of average time constant $\bar{\tau}_e$ for body A as

$$\bar{\tau}_e = \frac{4}{\pi^2}\frac{V\rho c}{\bar{C}} = \frac{4}{\pi^2}\frac{\lambda}{\bar{C}}, \tag{16}$$

where subscript 'e' stands for estimated. Hence, Eq. (16) gives an expression which estimates average transient response just by using a steady state analysis. However, it is important to note that the described estimation gives only a lumped measure of the time constant averaged over the entire body and hence, does not provide local information within the considered domain. Therefore, we typically divide a design into a number of sub-geometries each of which is characterized by a $\bar{\tau}_e$ value. Also, in order to make this calculation invariant of domain size, a normalized time constant is considered as explained in the next section.

METHODOLOGY

The conceptual understanding described in the previous section is utilized for analyzing sub geometries within a given AM design. For this purpose, the spatial domain is divided into a number of cells, as shown in Fig. 3(a). An enlarged view of one of the cells within the geometry is separately shown in Fig. 3(b). Figure 3(c) shows the finite element mesh for this cell along with the boundary conditions which remains same as described for defining thermal conductance. A steady state thermal analysis is carried out using FEA by solving the heat equation given as

$$\frac{\partial^2 T}{\partial x^2} + \frac{\partial^2 T}{\partial y^2} = 0. \tag{17}$$

This gives a temperature field, as shown in Fig. 3(d). Average conductance $\bar{C}$ is calculated for each cell using Eq. (2) which is used for estimating the time constant using Eq. (16). The thermal time constant obtained from this analysis is utilized as a quantifier of heat accumulation for the geometry enclosed in that cell.

In order to verify the proposed formulation based on computationally cheap steady-state analysis, a transient heating response for each cell geometry is also computed through FEA which gives a temperature distribution as a function of time $T(x, y, t)$. A time step of 1s is considered for a total analysis time of 20s. Average temperature $\bar{T}(t)$ for each time step is calculated using Eq. (3)

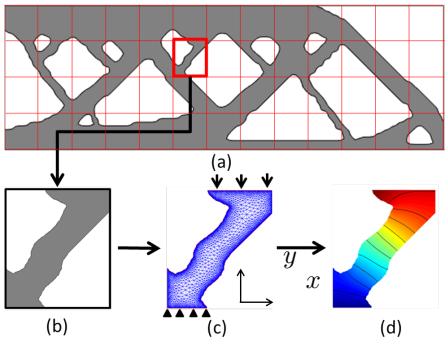

FIGURE 3. (a) A 2D geometry discretized into rectangular cells, (b) sample cell geometry, (c) meshing, (d) temperature field.

and fitted to the function

$$\bar{T}(t) = \bar{T}_{ss}(1 - e^{-\frac{t}{\bar{\tau}_r}}), \tag{18}$$

and a reference time constant $\bar{\tau}_r$ is determined for each cell according to the best fit. Reference and estimated time constants are represented as $\bar{\tau}_r$ and $\bar{\tau}_e$, respectively. In order to make the proposed methodology less sensitive to the cell size, normalized time constants are considered by dividing both time constants with that of a solid cell. Eq. (11) is used for calculating time constant for solid cell. Estimated $\bar{\tau}_e$ and reference $\bar{\tau}_r$ time constant maps for the design shown in Fig. 3(a) are presented in Fig. 4a and 4b, respectively. A cell-to-cell comparison is done between both the time constants, maximum and mean error is found to be 9.6% and 4.6%, respectively. Also, the steady state analysis is found to be 70% computationally cheaper than transient analysis. A schematic of the process for one of the cell geometry is presented in Fig. 5.

Concept of overlapping cells

The concept of dividing the design into overlapping cells has been utilized here in order to maximize the possibility of detecting heat accumulation zones. The design shown in Fig. 6 is first divided into a grid of $n_x \times n_y$ unit squares where n_x and n_y refers to number of grids in x and y directions, respectively. A cell is then defined with W_s unit squares in each direction as shown by cell A in Fig. 6. This cell is then moved by 1 unit in x and/or y directions in order to to define other possible cell geometries labeled as B and C, respectively. The process

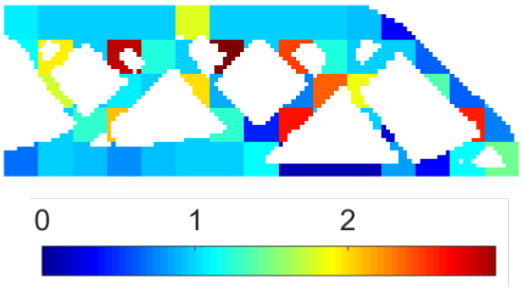

(a) Estimated time constant ($\bar{\tau}_e$) map

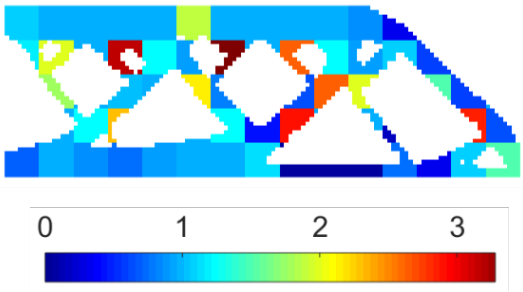

(b) Reference time constant ($\bar{\tau}_r$) map

FIGURE 4. Time constant maps for geometry shown in Fig. 3(a).

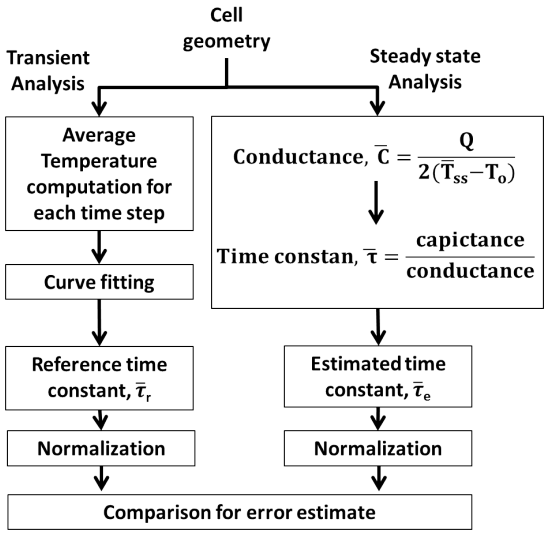

FIGURE 5. Flowchart for comparing reference $\bar{\tau}_r$ and estimated $\bar{\tau}_e$ time constant for each cell geometry obtained using transient and steady state thermal analysis, respectively.

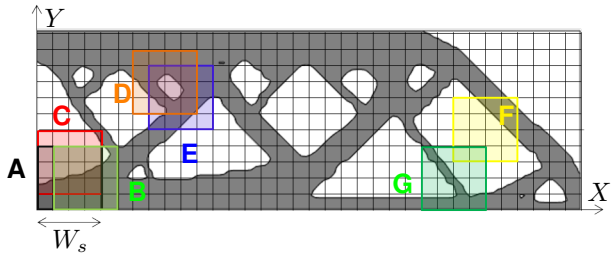

FIGURE 6. Definition of overlapping cells for heat accumulation detection.

is repeated such that all possible permutations $(n_x - W_s + 1)(n_y - W_s + 1)$ are considered for positioning the cell and defining cell geometries. A few of such possible cells are shown (labeled as A to G) in Fig. 6. The motivation behind considering all possible cell positions is to examine every possible geometry configuration (within the given grid resolution) for estimating highest time constants and hence, enhance the probability of heat accumulation detection.

NUMERICAL EXAMPLE

This section presents the implementation of the above discussed concepts for the purpose of detecting heat accumulation zones within the design shown in Fig. 6. Estimated time constants ($\bar{\tau}_e$) and reference time constants ($\bar{\tau}_r$) are calculated for each cell and Fig. 7a and 7b show the time constant map. Here, a cell overlaps its neighbors if its time constant is higher than that of adjacent cells. A cell-to-cell comparison between estimated and reference time constants is done and maximum and mean error is found to be 15.3% and 4.7% respectively. A computational gain of 75% is achieved by using steady state instead of transient analysis. Table 1 presents the parameters and material properties used for this analysis.

TABLE 1. Parameters for heat accumulation detection

Parameter	Value
Conductivity	7.1 W/m-K
Density	4.4×10^3 Kg/m^3
Specific heat	553 J/Kg-K
n_x	120
n_y	40
W_s	5

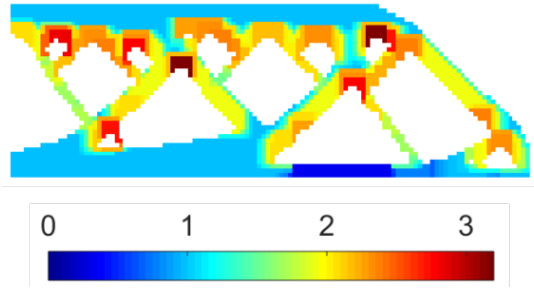

(a) Estimated time constant ($\bar{\tau}_e$) map obtained by steady state analysis.

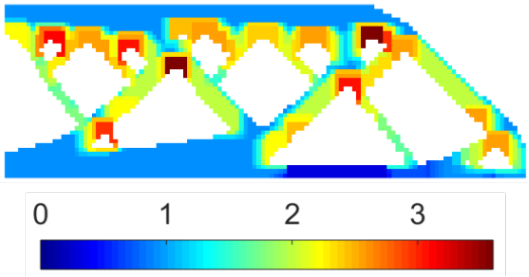

(b) Reference time constant ($\bar{\tau}_r$) map obtained by transient analysis.

FIGURE 7. Time constant maps obtained by the heat accumulation scheme using the concept of overlapping cells.

OBSERVATIONS

As seen in Fig. 7, high time constants are recorded close to overhang surfaces. More importantly, it is noteworthy that Cells D, E, G and F shown in Fig. 6 have a cell geometry with 45° overhang angle. However, regions covered by Cells D and E tend to have a higher time constant than Cells G and F. This shows that heat accumulation for a design feature depends heavily on local geometry around its vicinity and purely geometric design guidelines of prescribing a limiting overhang value might become insufficient for preventing problems associated with local heat accumulation. This justifies development of design methods which can address physics of the manufacturing process in a more comprehensive manner and thus, can be advantageous for precision AM industry.

CONCLUSIONS AND FUTURE WORK

A simplification approach has been proposed for identification of heat accumulation zones in an AM part. The method employs steady state thermal analysis for predicting heat accumulation within local regions of a given AM design. Information from local geometries is then assembled and presented in form of a time constant map which gives a pictorial representation of heat accumulation behavior for the entire structure. A transient analysis is also carried out to verify the developed analytical understanding and errors in estimation are reported along with achieved computational gain. It is found that heat accumulation tendency of a design feature is related to the local geometry around it and hence, a geometric design guideline only limiting the overhang angle can become insufficient in certain regions.

The computational advantage offered by the proposed method enables development of a physics based topology optimization method which would be beneficial for designing precision AM components. Next step for this research is to combine the developed method with density based topology optimization by penalizing design features which are prone to heat accumulation during each iteration.

REFERENCES

[1] Sames WJ, List F, Pannala S, Dehoff RR, Babu SS. The metallurgy and processing science of metal additive manufacturing. International Materials Reviews. 2016;61(5):315–360.

[2] Ranjan R, Yang Y, Ayas C, Langelaar M, Van Keulen F. Controlling local overheating in topology optimization for additive manufacturing. In: Proceedings of euspen special interest group meeting: additive manufacturing, Leuven, Belgium; 2017.

[3] Schoinochoritis B, Chantzis D, Salonitis K. Simulation of metallic powder bed additive manufacturing processes with the finite element method: A critical review. Proceedings of the Institution of Mechanical Engineers, Part B: Journal of Engineering Manufacture. 2017;231(1):96–117.

[4] Keller N, Ploshikhin V. New method for fast predictions of residual stress and distortion of AM parts. In: Solid Freeform Fabrication Symposium; 2014. p. 1229–1237.

[5] ASTM C168 - Terminology Relating to Thermal Insulation. ASTM International, West Conshohocken, PA, USA; 2013.

[6] Kobryn PA, Semiatin S. Microstructure and texture evolution during solidification processing of Ti–6Al–4V. Journal of Materials Processing Technology. 2003;135(2-3):330–339.